Universal G ∼ L −3 law for the low-frequency shear modulus of confined liquids

Alessio Zaccone, Laurence Noirez

Universal $G' \sim L^{-3}$ law for the low-frequency shear modulus of confined liquids

Alessio Zaccone*,†,‡,¶ and Laurence Noirez*,§

†*Department of Physics "A. Pontremoli", University of Milan, 20133 Milan, Italy*

‡*Department of Chemical Engineering and Biotechnology, University of Cambridge, CB30AS Cambridge, U.K.*

¶*Cavendish Laboratory, University of Cambridge, CB30HE Cambridge, U.K.*

§*Laboratoire Léon Brillouin (CEA-CNRS), Univ. Paris-Saclay, CEA-Saclay, 91191 Gif-sur-Yvette, France*

E-mail: alessio.zaccone@unimi.it; laurence.noirez@cea.fr

Abstract

Microfluidic and nanofluidic technologies have asserted themselves as new paradigms which have radically boomed activities dedicated to the chemical, bio-analysis and biomedical sectors. In spite of intense technological development, the fundamental physico-chemical properties of liquids confined on sub-millimeter scales have remained poorly understood. One of the most striking effects is the large elasticity (and viscosity) of confined liquids, which grows upon further decreasing the confinement length, L. Liquids under sub-millimeter confinement display a low-frequency shear modulus in the order of $1 - 10^3$ Pa, contrary to our everyday experience of liquids as bodies with a zero low-frequency shear modulus. While early experimental evidence of this effect (starting with Boris Derjaguin's work) was met with skepticism due to its counter-intuitive character and abandoned, further experimental results and most recently a

new atomistic theoretical framework have confirmed that liquids indeed possess a finite low-frequency shear modulus G' and that this scales with the inverse cubic power of confinement length L. After a brief historical overview and an introduction to the theoretical description of this effect, we show that this law is universal by analyzing experimental data on a wide range of materials (water, glycerol, ionic liquids, non-entangled polymer liquids, isotropic liquids crystals). Open questions and potential applications in mechanochemistry, energy and other fields are highlighted in conclusion.

Introduction

Our daily life experience and education tell us that when a liquid, e.g. liquid water, is subjected to an infinitesimal shear stress, it flows. In physics, the absence of noticeable mechanical resistance can be expressed by saying that the shear elastic modulus G of liquids is identically zero, where the shear modulus represents the proportionality coefficient between the applied shear stress (σ) and the resulting deformation of a solid body (γ), i.e. Hooke's law $\sigma = G\gamma$. Here a first important distinction comes into play, as the above statement is true for nearly static measurements; i.e. at low-frequency, or low-deformation rate, where the shear modulus is zero, but at high frequency or high rate of deformation the shear modulus of liquids is large (as one would experience by diving into a swimming pool from a considerable height, a possibly painful experience if one is not an experienced diver!). This observation reflects the fact that liquids at high frequency of external drive behave like amorphous solids (e.g. glasses), because the atoms or molecules are made to oscillate at such high speed by the external field that they cannot escape the liquid cage made by their nearest neighbours. This goes along with the ability of liquids to sustain transverse acoustic waves at sufficiently high momenta or high frequencies, as predicted in early work by Yakov Frenkel in the 1940s.[1]

Besides this basic notion which defines the essential property of a liquid, our understanding of the physics of liquids is incomplete.[2] This is due to the fact that atoms and molecules

in a liquid are in a state of disorder and random motions, which is very different from that of atoms or molecules sitting on a regular lattice in crystalline solids. Therefore, it is difficult to find a mathematical description of the atomic or the molecular dynamics in a liquid, from which quantitative explanations of the macroscopic properties of liquids could be deduced.

As a consequence of this state of affairs, it has been impossible so far to rationalize the mechanics of liquids on microscopic scales. Already in 1989-1990, using the newly developed piezo-quartz resonance device, it has been experimentally observed, that a liquid film confined at several microns scale exhibits an unexpected shear elasticity at low frequency/rate of deformation, a behaviour much more akin to solids than to liquids.[3,4] In spite of the fact that these experiments were led by Boris Derjaguin, one of the most prominent Russian physicochemists of the 20th century, the observation was met with skepticism and abandoned by the scientific community because of the preconceived notion that liquids must have a zero shear modulus. From the early 2000s, many other experiments conducted by different teams, however, resulted in the same observation extending the identification of the "Derjaguin" shear elasticity up to the millimeter scale,[5] using different experimental techniques and different liquids (from liquid water to liquid crystals to ionic liquids and polymers).[6–12] A theoretical explanation for these phenomena, however, has remained elusive (despite the keen interest by Nobel laureate Pierre-Gilles de Gennes, a former colleague of one of us, right before his untimely death in 2007).

In Figure 1 the typical viscoelastic response of a sub-millimeter confined liquid is shown, in terms of the storage shear modulus $G'(\omega)$ and the dissipative loss modulus $G''(\omega)$, which represent, respectively, the real and imaginary part of the complex shear modulus $G^* = G'(\omega)+iG''(\omega)$. Here , ω is the frequency of the externally applied mechanical oscillation field (oscillatory strain), $\gamma = \gamma_0 \sin(\omega t)$, which triggers, under conditions of the linear response, a stress response $\sigma = \sigma_0 \sin(\omega t + \delta)$, where δ is a phase which is $\delta = 0$ for perfectly elastic response (Hooke's law) and $\delta = \pi/2$ for perfectly fluid response. The situation is summarized in Fig. 1(a). Experimentally, the solid-like response displays $G' > G''$, and a flat plateau of G'

at low frequency. The hallmark of liquid-like viscous response, instead, is that $G' \ll G'' = \eta\omega$ (where η is the shear viscosity), at low-frequency. While bulk liquids have $\delta = \pi/2$ (perfectly viscous response) for low frequencies of oscillation (typically in the range 0.001-10Hz), liquids in confined geometry and/or strongly in interaction with the substrate (wetting conditions) may display δ values much smaller than $\pi/2$, which indicates a solid-like viscoelastic response. This goes along with a substantial low-frequency plateau value of storage modulus, $G' > G''$. An experimental example which illustrates the solid-like response of confined liquids is provided in Fig. 1(c)-(d), showing the mechanical response of a small molecule liquid, glycerol, at low frequency and room temperature. Among other simple liquids, very similar mechanical response at low frequency has been measured for water,[6] for ortho-terphenyl (OTP)[7] and for ionic liquids.[8] Similar solid-like properties have also been observed with higher-molecular weight liquids, such as linear alkanes,[9] isotropic liquids crystals,[10] side-chain liquid crystals,[11,12] entangled[7] and non-entangled polymers.[10,13] The same phenomena have also been observed at the nanoscale in nano-confined liquids.[14–16]

It is important to note the role of boundary conditions, i.e. of the surface treatment. For certain solid surfaces in direct contact with the liquid, the liquid molecules are firmly anchored to the solid surface. This is typically associated with high wettability or wetting of the surface, and implies strong attractive interaction between the liquid molecules and the surface. These conditions are complex involving the surface energy of the solid in addition to cleaned, atomically smooth conditions. If that is not the case, e.g. for non-wetting surfaces, the liquid molecules in direct contact with the surface are instead more free in their relative motion with respect to the solid surface. This makes a big difference for the conditions to access the viscoelastic response. It turns out that, in the case of wetting surfaces, the mechanical response of the confined liquid is solid-like, whereas for non-wetting surfaces, the standard purely viscous response is observed. This phenomenon can be mechanistically explained in terms of plane-wave null boundary conditions for the wetting surfaces (or absence thereof, for non-wetting surfaces) in the following theoretical analysis.

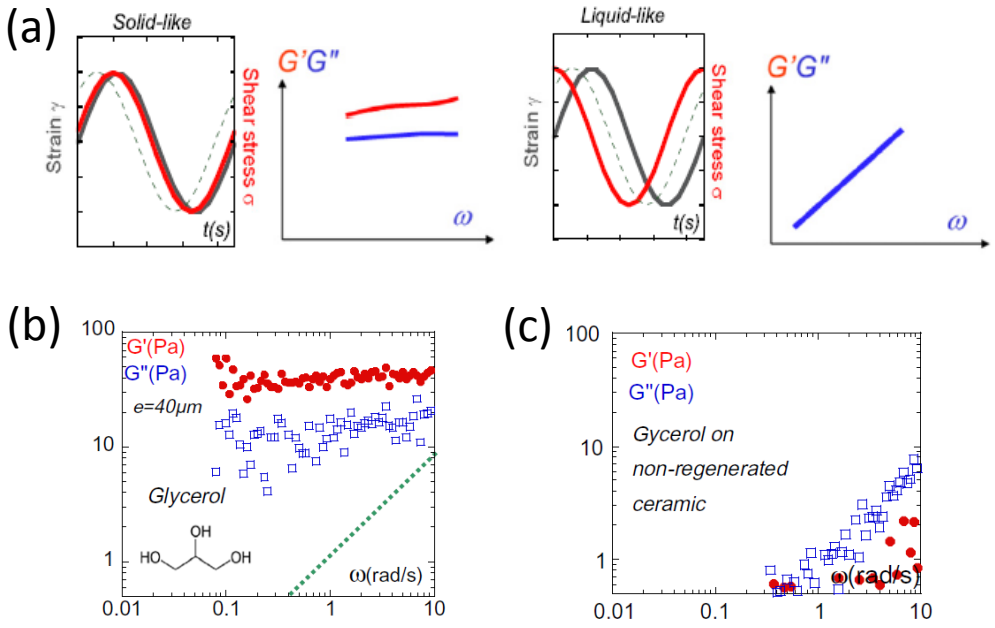

Figure 1: Dynamic viscoelastic response of liquids. Panel (a) shows schematic depiction of time dependent shear stress σ and shear strain γ for solid-like (left) and liquid-like (right) systems and the corresponding frequency dependent viscoelastic curves. The lower set of figures shows the experimentally measured G' and G'' as a function of oscillation frequency ω for glycerol in good (cleaned/thermally regenerated ceramic), panel (b), and poor (non-cleaned ceramic) surface-wetting conditions, panel (c). Panel (b) obtained using a surface state perfectly free of impurities, displays higher viscoelastic moduli and leads to $G' > G''$ indicating a solid-like response. In panel (c), where the thermal regeneration of the surfaces has not been applied (hence causing a lower energy of adhesion, thus poor wetting and possibly de-wetting) the G'' scales exactly linear with ω, in line with expectations for purely viscous liquids. Reproduced with permission of Elsevier from Ref.[17]

.

These experimental findings have recently been rationalized from the point of view of theory. Theories of liquids have normally focused on the high-frequency shear modulus for which atomistic or molecular-level expressions are available, such as the Mountain-Zwanzig formula,[18] precisely because the low-frequency mechanical of bulk liquids is not supposed to exist. In the allied field of amorphous solids, such as glasses, instead, the mechanical response has been studied across the entire frequency range, since amorphous solids obviously exhibit a finite zero-frequency shear modulus. In particular, lattice dynamics can be extended to deal with disordered systems where the positions of atoms/molecules are completely random, to arrive at theoretical expressions for the elastic constants and for the viscoleastic moduli.[19] The resulting theoretical framework is sometimes referred to as nonaffine lattice dynamics or NALD.[20,21] The theory has proved effective in quantitatively describing elastic, viscoelastic and plastic response of systems as diverse as jammed random packings and random networks,[19] glassy polymers,[22–24] metallic glass,[25] and colloidal glasses.[26] Furthermore, NALD intrinsically takes into account long-range correlation phenomena[27,28] that are present also in liquids and give rise to acoustic wave propagation.

The usual starting point is the equation of motion of a microscopic building block, i.e. an atom or a molecule for atomic liquids or molecular liquids, respectively. In the case of polymers, the building block could be identified with a monomer of the polymer chain.[22] Following previous literature,[19,20] we introduce the Hessian matrix of the system $\underline{\underline{H}}_{ij} = -\partial^2\mathcal{U}/\partial\mathring{\underline{q}}_i\partial\mathring{\underline{q}}_j$ and the affine force field $\underline{\underline{\Xi}}_{i,\kappa\chi} = \partial\underline{f}_i/\partial\eta_{\kappa\chi}$, where $\eta_{\kappa\chi}$ is the strain tensor. For example, for simple shear deformation the xy entry of tensor $\eta_{\kappa\chi}$ is given by a scalar γ, which coincides with the angle of deformation.

Furthermore, $\mathring{q}_i$ is the coordinate of atom i in the initial undeformed frame (denoted with the ring notation), while $\underline{f}_i = \partial\mathcal{U}/\partial\underline{q}_i$ denotes the force acting on atom i in the affine position, i.e. in the initial frame acted upon by the macroscopic deformation (see Fig. 2(a) for a visual representation of affine positions in a deformed frame), hence the name "affine" force-field. Greek indices refer to Cartesian components of the macroscopic deformation (e.g.

$\kappa\chi = xy$ for shear). For a liquid, the Hessian $\underline{\underline{H}}_{ij}$ is normally evaluated in a reference state obtained from averaging over MD configurations to include instantaneous normal modes or INMs (purely imaginary vibrational frequencies).[22] For more details about INMs see Ref.[29]

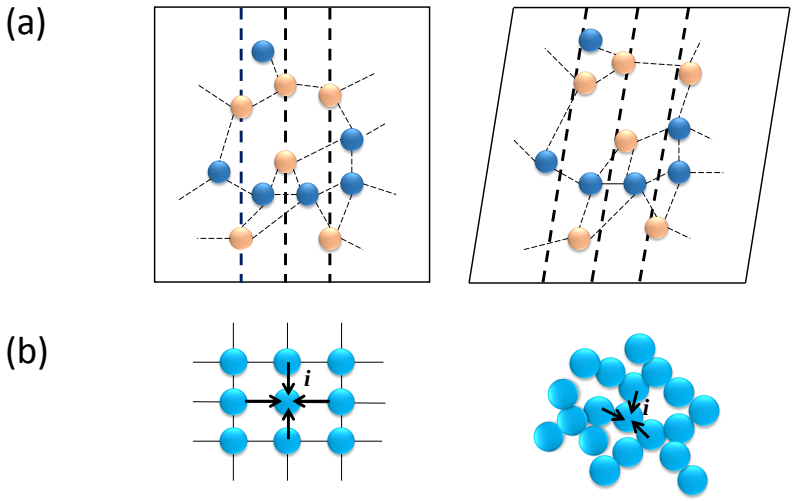

Figure 2: Schematic illustration of nonaffine displacements in amorphous media. Panel (a) shows the rearrangements or displacements of atoms upon application of an external shear strain. If the deformation were affine, atoms which sit exactly on the dashed lines in the underformed frame (left) would still sit exactly on dashed lines also in the deformed frame (right). However, in a disordered environment this does not happen, and in the deformed frame the atoms that were sitting on the dashed lines in the undeformed frame are no longer sitting on the dashed lines, but are displaced from them. The distance from the actual positions of the atoms to the dashed line corresponds to the nonaffine displacements. Panel (b) provides a visual explanation of the origin of nonaffine displacements in disordered environments. Left figure shows a perfect lattice where upon applying a small deformation the nearest-neighbour forces from surrounding atoms cancel each other out in the affine positions, so there is no need for nonaffine displacements to arise. In the right figure, instead, the tagged atom i is not a center of inversion symmetry, which implies that nearest-neighbour forces from surrounding atoms do not balance in the affine position, hence a net force arises which triggers the nonaffine displacement in order to maintain mechanical equilibrium.

As shown in previous works, the equation of motion of atom i in a disordered medium subjected to an external strain, in mass-rescaled coordinates, can be written:[20,22]

$$\frac{d^2\underline{x}_i}{dt^2} + \nu\frac{d\underline{x}_i}{dt}dt + \underline{\underline{H}}_{ij}\underline{x}_j = \underline{\underline{\Xi}}_{i,\kappa\chi}\eta_{\kappa\chi} \tag{1}$$

where $\underline{\underline{\eta}}$ is the Green-Saint Venant strain tensor and ν is a microscopic friction coefficient

which arises from long-range dynamical coupling between atoms mediated by anharmonicity of the pair potential. The term on the r.h.s. physically represents the effect of the disordered (non-centrosymmetric) environment leading to nonaffine motions: a net force acts on atom i in the affine position (i.e. the position prescribed by the external strain tensor $\eta_{\kappa\chi}$). The situation is schematically depicted in Fig. 2(b), which contrasts a centrosymmetric environment (left panel), where all atoms are at mechanical equilibrium even in the affine position (here for an infinitesimal strain) due to cancellation of nearest-neighbour forces that are mirror-image of each other across the central particle, with the situation in a disordered system (liquid or amorphous solid) in the right panel. In the latter case, the nearest-neighbour forces do not cancel thus leading to a net force acting on the central atom.

As a consequence, in order to keep mechanical equilibrium on all atoms throughout the deformation, an additional *nonaffine* displacement is required in order to relax the force f_i acting in the affine position. This displacement brings each atom i to a new (nonaffine) position. A schematic depiction of a nonaffine displacement is shown in Fig.2(a).

The equation of motion Eq. 1 can also be derived from first principles, from a model particle-bath Hamiltonian as shown in previous work.[22] Using standard manipulations (Fourier transformation and eigenmode decomposition from time to eigenfrequency[20]), and applying the definition of mechanical stress, we obtain the following expression for the viscoelastic (complex) elastic constants:[20,22]

$$C_{\alpha\beta\kappa\chi}(\omega) = C^{Born}_{\alpha\beta\kappa\chi} - \frac{1}{V}\sum_n \frac{\hat{\Xi}_{n,\alpha\beta}\hat{\Xi}_{n,\kappa\chi}}{\omega^2_{p,n} - \omega^2 + i\omega\nu} \tag{2}$$

where $C^{Born}_{\alpha\beta\kappa\chi}$ is the Born or affine part of the elastic constant, i.e. what survives in the high-frequency limit. Here, ω represents the oscillation frequency of the external strain field, whereas ω_p denotes the internal eigenfrequency of the liquid (which results, e.g., from diagonalization of the Hessian matrix[22]). We use the notation ω_p to differentiate the eigenfrequency from the external oscillation frequency ω.

As already mentioned above, an atomistic expression for $G_\infty \equiv C_{xyxy}^{Born}$ is provided by the well known Zwanzig-Mountain (ZM) formula,[18] in terms of the pair potential $V(r)$ and the radial distribution function $g(r)$. The sum over n in Eq.(2) runs over all $3N$ degrees of freedom (given by the atomic or molecular building blocks with central-force interactions). Also, we recognize the typical form of a Green's function, with an imaginary part given by damping and poles $\omega_{p,n}$ that correspond to the eigenfrequencies of the excitations.

At this point we use a key assumption of plane waves, i.e. we assume that at low values of wavevector k (i.e. for long wavelengths λ), liquids can support shear elastic waves. Propagation of longitudinal acoustic waves in liquids is of course a well known fact to everyone who does snorkeling or swims under the water level, with firmly established both experimental and theoretical evidence of longitudinal acoustic dispersion relations.[30–32] For transverse or shear acoustic waves in liquids, instead, there is no propagation below a characteristic wavenumber. Indeed, there is an onset value of k, that we shall denote k_g, above which these modes can propagate in liquids, known as the k-gap,[2] again a result due originally to Frenkel,[1] and recently demonstrated by Trachenko and co-workers.[33,34]

Following the analytical steps presented in Ref.,[35] we arrive at the following expression for the frequency-dependent storage modulus G',

$$\begin{aligned} G^*(\omega) =& G_\infty - B\int_{\frac{1}{L}}^{k_D} \frac{\omega_{p,L}^2(k)}{\omega_{p,L}^2(k) - \omega^2 + i\omega\nu} k^2 dk \\ & - B\int_{k_{min}}^{k_D} \frac{\omega_{p,T}^2(k)}{\omega_{p,T}^2(k) - \omega^2 + i\omega\nu} k^2 dk, \end{aligned} \tag{3}$$

where the first integral represents the nonaffine (negative or softening) contribution due to longitudinal (L) acoustic modes, while the second integral represents the nonaffine (also softening) contribution due to the transverse (T) acoustic modes. In the above expression, $k_{min} = \max\left(k_g, \frac{1}{L}\right)$ is an "infrared" cutoff for the transverse modes, with k_g the onset wavenumber for transverse phonons in liquids (the k-gap), and L the confinement length. In the above treatment, the assumption of plane waves in 3D implies the condition

$\sqrt{k_x^2+k_y^2+k_z^2}=k=2\pi/\lambda$, which leads to the spherical integrals of Eq. 3, with the metric factor k^2.

For the longitudinal modes, one can resort to the Hubbard-Beeby theory of collective longitudinal modes in liquids,[30] which has been shown to provide a good description of experimental data, and thus use Eq. (43) from Ref.[30] for $\omega_{p,L}(k)$ inside the integral above. As shown in Ref.,[35] the final result for the low-frequency G' does not depend on the form of the $\omega_{p,L}(k)$ dispersion relation. However, for the mathematical completeness of the theory it is important to specify which analytical forms for the dispersion relations can be used.

Anyway, upon taking the real part of G^*, which gives the storage modulus G', and focusing on low external oscillation frequencies $\omega \ll \omega_p$ used experimentally, in both integrals numerator and denominator cancel out, leaving the same expression in both integrals. Therefore, as anticipated above, the final low-frequency result does not depend on the actual form of $\omega_{p,L}(k)$, nor of $\omega_{p,T}(k)$, although the latter, due to the k-gap, plays an important role (see the expression for k_{min} above) in controlling the "infrared" cutoff of the transverse integral. In the experiments where the size effect of confinement is seen, $k_g \ll \frac{1}{L}$,[36] and $k_{min}=\frac{1}{L}$, thus leading to

$$G'=G_\infty-\alpha\int_{1/L}^{k_D}k^2dk=G_\infty-\frac{\alpha}{3}k_D^3+\frac{\beta}{3}L^{-3}. \tag{4}$$

For the lower limit of the nonaffine integral we used an infrared cutoff

$$k_{min}\equiv|\mathbf{k}_{min}|=2\pi\sqrt{(1/L_x)^2+(1/L_y)^2+(1/L)^2}. \tag{5}$$

Upon assuming that the liquid is confined in the z direction, such that $L\equiv L_z \ll L_x, L_y$, the lower limit in the nonaffine integral over k-space thus reduces to $1/L$, as displayed in Eq. 4.

In Eq. 4, the only term which depends on the system size is the last term, while α, β are numerical prefactors. In liquids that are in thermodynamic equilibrium, a different version of the nonaffine response formalism called stress-fluctuation formalism can be used (the two versions have been shown to be equivalent in Ref.[37]) in combination with standard equilibrium

statistical mechanics. It has been shown in Ref.[38] that the affine or high-frequency (Born) term G_∞ and the negative nonaffine term (here, $-\frac{\alpha}{3}k_D^3$) cancel each other out exactly, such that $G'(\omega \to 0) = 0$ for $L \to \infty$ (bulk liquids). Therefore, for liquids under sub-millimeter confinement, only the third term in the above equation survives, and we finally obtain

$$G' \approx \beta' L^{-3} \tag{6}$$

where $\beta' = \beta/3$ is a numerical prefactor. This law has been derived for the first time in Ref.[35] It is worth noticing that G_∞ is independent of L. This fact can be seen, e.g. through the Zwanzig-Mountain formula where the main contribution to G_∞ is given as an integral that contains $dV(r)/dr$ as a multiplying factor in the integrand, with $dV(r)/dr = 0$ after few molecular diameters. This, in turn, implies that no dependencies on length-scales much larger than the nearest-neighbour cage can be present in G_∞.

The above theory clarifies that the liquid confinement between two plates is able to "remove" certain low-frequency normal mode collective oscillations of molecules, associated with the nonaffine motions (i.e. negative contributions to the elasticity), which are responsible for the fluid response of liquids under standard macroscopic ("unconfined") conditions. These motions are responsible for reducing the shear modulus basically to zero in macroscopic liquids. Under confinement, instead, the shear modulus is non-zero because these collective oscillations modes are suppressed, and the theory of Zaccone and Trachenko[35] provides the universal law by which the shear modulus grows upon reducing the confinement (gap) size. In particular, the static shear modulus grows with the inverse cubic power of the gap size.

In Ref.,[35] the law $G' \sim L^{-3}$ was found to provide a perfect description of experimental data measured in an isotropic liquid crystal system ($PAOCH_3$) upon varying the confinement length using a conventional rheometer. Here, we show that this law is truly universal and we present theoretical fittings of several, very different, systems in Fig. 3.

In all these systems, i.e. short chain polymers, isotropic liquid crystals, ionic liquids

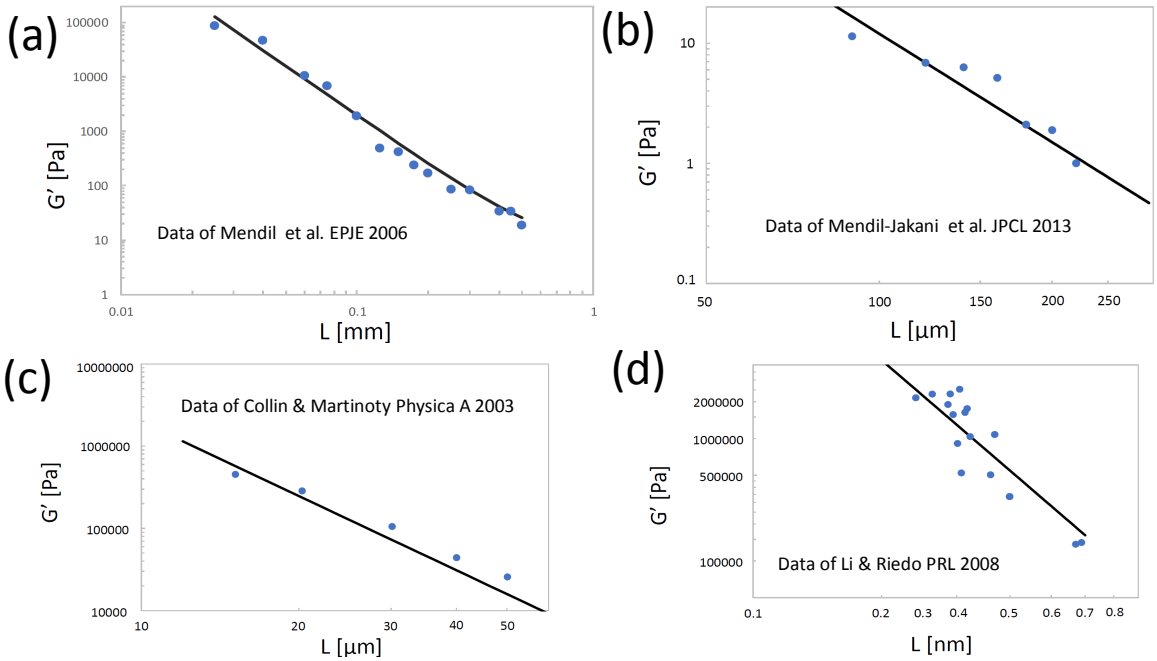

Figure 3: Experimental data of low-frequency shear modulus G' versus confinement length L for different systems, where circles represent experimental data while the solid line is the law $G' \sim L^{-3}$ derived in Ref.[35] (a) shows the comparison for $PAOCH_3$, an isotropic liquid crystal system from Ref.;[10] (b) shows the same comparison for ionic liquids, from Ref.;[8] (c) shows experimental data for short-chain (non-entangled) polystyrene melts from Ref.;[13] (d) shows experimental data for nanoconfined water from Ref.[14]

and even nano-confined water, the law Eq. 6 appears robust, as shown in Fig. 3. In the case of nano-confined water[14] one would expect a crossover from $\sim L^{-3}$ into a L^{-1} regime once that a 2D monolayer is reached. This is expected because the k-space integral in Eq. 4 contains a metric factor k in 2D, instead of k^2 for 3D (in fact, k^{d-1} for generic d-dimensional space). This crossover is not seen in the data of Fig. 3(d), which calls for further investigations, both experimentally and theoretically. Experimental data have also been reported for ortho-terphenyl (OTP), an organic liquid (data not shown here). Those data also show the $\sim L^{-3}$ behaviour, but the data at shortest confinement length, $\sim 0.01mm$, suggest the possible existence of a plateau upon going towards lower L, while the experimental accuracy lowers as the confinement increases. The paucity of experimental data does not allow for drawing a definitive conclusion on this effect (i.e. the possible existence of a plateau in G' at low L in certain systems), which should also be the object of further investigation, both experimentally and in theory.

As mentioned earlier, a crucial role is played by the surface anchoring. The solid-like response of confined liquids is indeed observed mainly for atomically smooth surfaces (crystal planes) or for conditions of good wetting between liquid and solid surface (high energy surfaces). Instead, a standard purely viscous response is reported for non-wetting or poorly wetting surfaces; see Fig. 4 for a schematic illustration of two different surface wetting conditions. The same observation has been made in the case of nano-confined water, with a substantially higher viscosity measured in the case of good wetting in Ref.[15]

From the theoretical point of view, this fact can be explained by referring to the nonaffine lattice dynamic framework summarized above. In particular, wettability connects with the assumption of plane waves and with the implicit *null boundary conditions* for the displacement field of plane waves. This leads straightforward to the term $\sim L^{-3}$ in Eq. 4 above, which is the term responsible for the solid-like elastic response. Without the full wetting boundary conditions between the liquid and the solid surface, the liquid molecules would not be well-anchored to the solid surface, so the null boundary condition for the acoustic waves

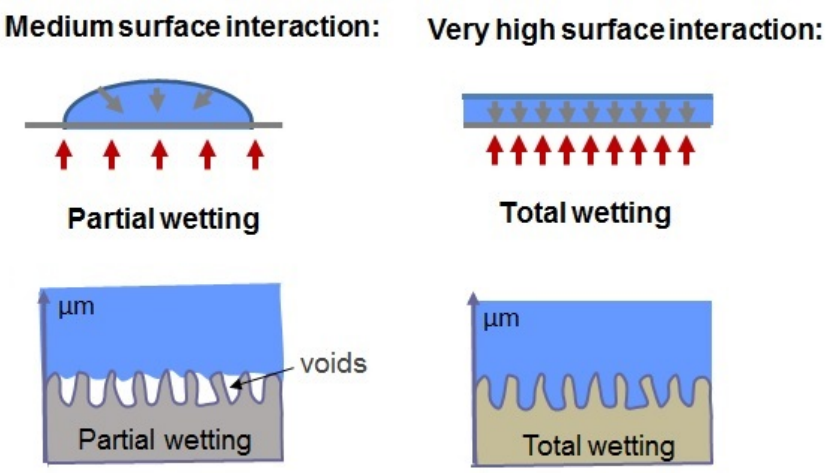

Figure 4: Schematic illustration of different levels of surface interaction between liquid molecules and solid substrate. A not so strong attractive interaction leads to partial wetting (left panel), whereas a strong attractive interaction with the solid surface leads to total wetting filling in the rough edges (right panel).

would not apply, and the very existence of elastic plane waves would then be called into question. Certainly, the above theoretical framework would not be applicable in that case as it relies on the ability of the liquid to support plane waves. We can speculate that when molecules are not anchored to the solid surface, the effective "removal" of softening nonaffine motions due to confinement is less effective, hence the rigidifying effect of "cutting" nonaffine motions off due to confinement would not be active. A more precise explanation may require a different theoretical approach, possibly working in eigenfrequency domain rather than in k-space, and is an interesting problem for future research.

A number of outstanding questions remain open for future investigations. For example, it could be interesting to explore what kind of connection exists between the above scenario of solid-like elasticity of confined liquids and the glass transition under confinement. The latter is an intensively studied problem, especially in the context of thin polymer films.[39,40] Another important issue, is the progress that can be done with numerical simulations. In molecular dynamics (MD), the shear modulus of a confined liquid can be measured but the noise is currently too large (since the size MD simulated systems is small) to make predictions for most realistic situations.[41] Another issue is represented by the small time-step used espe-

cially in atomistic simulations (on the order of femtoseconds), which prevents accessing the low-frequency shear modulus. Quasi-static deformation methods implemented atomistically could be a step forward but they have not demonstrated quantitative predictive power thus far, in comparison with experiments. Also, the power-law nature of the relation $G' \sim L^{-3}$ implies the absence of characteristic length-scales (typical of power-laws), which suggests that the same mechanisms apply at different length-scales, i.e. the same laws apply with L being in the sub-millimeter, micron or nano-scale. Similarities between trends observed for sub-millimeter[10] and nano-confined fluids,[14,15] both in terms of solid-like mechanical properties and role of wetting,[42] suggest that this may indeed be the case, but further research is required to more firmly establish a complete multi-scale framework.

The potential applications of solid-like elasticity of confined liquids, and its tuneability via the control and modulation of the interfacial energy and gap size L, are manifold, encompassing fields as diverse as mechanical stress-assisted manipulation of soft and biological matter in microfluidics,[43?] protective equipment,[44] biomedical flow applications,[45] oil recovery,[46] and heat transfer in microengineering applications. Recently, it has been demonstrated that the thermal response of confined liquids is very similar to that of solids,[47] which opens up new opportunities for exploiting thermoelasticity of confined fluids, e.g. for energy conversion.

Finally, another potential exciting application of this effect is in the emerging field of mechanochemistry[48–51] and mechanobiology:[52] a (confined) liquid with a finite low-frequency shear modulus G' is able to support mechanical stress-transmission much more efficiently and with much lower dissipative losses compared to standard viscous liquids. This fact may open up new avenues for mechanically-induced enhancement of chemical reaction kinetics, by combining the force-transmission efficiency typical of elastic solids with all the favourable solvation and solubility properties of liquids.[53–56]

Acknowledgement

AZ thanks Kostya Trachenko, Ivan Kriuchevskyi and Giancarlo Ruocco for enlightening discussions. AZ acknowledges financial support from US Army Research Office

References

(1) Frenkel, J. *Kinetic Theory of Liquids*; Oxford University Press, Oxford, 1946.

(2) Trachenko, K.; Brazhkin, V. V. Collective modes and thermodynamics of the liquid state. *Reports on Progress in Physics* **2015**, *79*, 016502.

(3) Derjaguin, B.; Bazaron, U.; Zandanova, K.; Budaev, O. The complex shear modulus of polymeric and small-molecule liquids. *Polymer* **1989**, *30*, 97 – 103.

(4) Derjaguin, B. V.; Bazaron, U. B.; Lamazhapova, K. D.; Tsidypov, B. D. Shear elasticity of low-viscosity liquids at low frequencies. *Phys. Rev. A* **1990**, *42*, 2255–2258.

(5) Noirez, L. Origin of shear-induced phase transitions in melts of liquid-crystal polymers. *Phys. Rev. E* **2005**, *72*, 051701.

(6) Noirez, L.; Baroni, P. Identification of a low-frequency elastic behaviour in liquid water. *Journal of Physics: Condensed Matter* **2012**, *24*, 372101.

(7) Noirez, L.; Mendil-Jakani, H.; Baroni, P. Identification of finite shear-elasticity in the liquid state of molecular and polymeric glass-formers. *Philosophical Magazine* **2011**, *91*, 1977–1986.

(8) Mendil-Jakani, H.; Baroni, P.; Noirez, L.; Chancelier, L.; Gebel, G. Highlighting a Solid-Like Behavior in Tri-octylmethylammonium Bis(trifluoromethanesulfonyl)imide. *Journal of Physical Chemistry Letters* **2013**, *4*, 3775–3778.

(9) Noirez, L.; Baroni, P.; Cao, H. Identification of Shear Elasticity at Low Frequency in Liquid n-Heptadecane, Liquid Water and RT-Ionic Liquids [emim][Tf2N]. *Journal of Molecular Liquids* **2012**, *176*, 71 – 75, Special Issue Dynamics and Phase Transition: Selected Papers on Molecular Liquids presented at the EMLG/JMLG 2011 Annual Meeting 11 - 15 September 2011.

(10) Mendil, H.; Baroni, P.; Noirez, L. Solid-like rheological response of non-entangled polymers in the molten state. *The European Physical Journal E* **2006**, *19*, 77–85.

(11) Gallani, J. L.; Hilliou, L.; Martinoty, P.; Keller, P. Abnormal viscoelastic behavior of side-chain liquid-crystal polymers. *Phys. Rev. Lett.* **1994**, *72*, 2109–2112.

(12) Martinoty, P.; Hilliou, L.; Mauzac, M.; Benguigui, L.; Collin, D. Side-Chain Liquid-Crystal Polymers: Gel-like Behavior below Their Gelation Points. *Macromolecules* **1999**, *32*, 1746–1752.

(13) Collin, D.; Martinoty, P. Dynamic macroscopic heterogeneities in a flexible linear polymer melt. *Physica A: Statistical Mechanics and its Applications* **2003**, *320*, 235 – 248.

(14) Li, T.-D.; Riedo, E. Nonlinear Viscoelastic Dynamics of Nanoconfined Wetting Liquids. *Phys. Rev. Lett.* **2008**, *100*, 106102.

(15) Ortiz-Young, D.; Chiu, H.-C.; Kim, S.; Voïtchovsky, K.; Riedo, E. The interplay between apparent viscosity and wettability in nanoconfined water. *Nature Communications* **2013**, *4*, 2482.

(16) Monet, G.; Paineau, E.; Chai, Z.; Amara, M. S.; Orecchini, A.; Jimenéz-Ruiz, M.; Ruiz-Caridad, A.; Fine, L.; Rouzière, S.; Liu, L.-M.; Teobaldi, G.; Rols, S.; Launois, P. Solid wetting-layers in inorganic nano-reactors: the water in imogolite nanotube case. *Nanoscale Adv.* **2020**, *2*, 1869–1877.

(17) Noirez, L.; Baroni, P. Revealing the solid-like nature of glycerol at ambient temperature. *Journal of Molecular Structure* **2010**, *972*, 16 – 21, Horizons in hydrogen bond research 2009.

(18) Zwanzig, R.; Mountain, R. D. High-frequency elastic moduli of simple fluids. *The Journal of Chemical Physics* **1965**, *43*, 4464–4471.

(19) Zaccone, A.; Scossa-Romano, E. Approximate analytical description of the nonaffine response of amorphous solids. *Phys. Rev. B* **2011**, *83*, 184205.

(20) Lemaître, A.; Maloney, C. Sum Rules for the Quasi-Static and Visco-Elastic Response of Disordered Solids at Zero Temperature. *Journal of Statistical Physics* **2006**, *123*, 415.

(21) Zaccone, A. Elastic Deformations in Covalent Amorphous Solids. *Modern Physics Letters B* **2013**, *27*, 1330002.

(22) Palyulin, V. V.; Ness, C.; Milkus, R.; Elder, R. M.; Sirk, T. W.; Zaccone, A. Parameter-free predictions of the viscoelastic response of glassy polymers from non-affine lattice dynamics. *Soft Matter* **2018**, *14*, 8475–8482.

(23) Ness, C.; Palyulin, V. V.; Milkus, R.; Elder, R.; Sirk, T.; Zaccone, A. Nonmonotonic dependence of polymer-glass mechanical response on chain bending stiffness. *Phys. Rev. E* **2017**, *96*, 030501.

(24) Elder, R. M.; Zaccone, A.; Sirk, T. W. Identifying Nonaffine Softening Modes in Glassy Polymer Networks: A Pathway to Chemical Design. *ACS Macro Letters* **2019**, *8*, 1160–1165.

(25) Zaccone, A.; Schall, P.; Terentjev, E. M. Microscopic origin of nonlinear nonaffine deformation in bulk metallic glasses. *Phys. Rev. B* **2014**, *90*, 140203.

(26) Laurati, M.; Maßhoff, P.; Mutch, K. J.; Egelhaaf, S. U.; Zaccone, A. Long-Lived Neighbors Determine the Rheological Response of Glasses. *Phys. Rev. Lett.* **2017**, *118*, 018002.

(27) Shelton, D. P. Long-range orientation correlation in water. *The Journal of Chemical Physics* **2014**, *141*, 224506.

(28) Zhang, Z.; Kob, W. Revealing the three-dimensional structure of liquids using four-point correlation functions. *Proceedings of the National Academy of Sciences* **2020**, *117*, 14032–14037.

(29) Stratt, R. M. The Instantaneous Normal Modes of Liquids. *Accounts of Chemical Research* **1995**, *28*, 201–207.

(30) Hubbard, J.; Beeby, J. L. Collective motion in liquids. *Journal of Physics C: Solid State Physics* **1969**, *2*, 556–571.

(31) Takeno, S.; Goda, M. A Theory of Phonon-Like Excitations in Non-Crystalline Solids and Liquids. *Progress of Theoretical Physics* **1972**, *47*, 790–806.

(32) Hansen, J.-P.; McDonald, I. R. *Theory of Simple Liquids*; Elsevier, Amsterdam, 2013.

(33) Yang, C.; Dove, M. T.; Brazhkin, V. V.; Trachenko, K. Emergence and Evolution of the k Gap in Spectra of Liquid and Supercritical States. *Phys. Rev. Lett.* **2017**, *118*, 215502.

(34) Khusnutdinoff, R. M.; Cockrell, C.; Dicks, O. A.; Jensen, A. C. S.; Le, M. D.; Wang, L.; Dove, M. T.; Mokshin, A. V.; Brazhkin, V. V.; Trachenko, K. Collective modes and gapped momentum states in liquid Ga: Experiment, theory, and simulation. *Phys. Rev. B* **2020**, *101*, 214312.

(35) Zaccone, A.; Trachenko, K. Explaining the low-frequency shear elasticity of confined liquids. *Proceedings of the National Academy of Sciences* **2020**, *117*, 19653–19655.

(36) Jackson, J. K.; De Rosa, M. E.; Winter, H. H. Molecular Weight Dependence of Relaxation Time Spectra for the Entanglement and Flow Behavior of Monodisperse Linear Flexible Polymers. *Macromolecules* **1994**, *27*, 2426–2431.

(37) Mizuno, H.; Silbert, L. E.; Sperl, M.; Mossa, S.; Barrat, J.-L. Cutoff nonlinearities in the low-temperature vibrations of glasses and crystals. *Phys. Rev. E* **2016**, *93*, 043314.

(38) Wittmer, J. P.; Xu, H.; Polińska, P.; Weysser, F.; Baschnagel, J. Shear modulus of simulated glass-forming model systems: Effects of boundary condition, temperature, and sampling time. *Journal of Chemical Physics* **2013**, *138*, 12A533.

(39) Napolitano, S.; Glynos, E.; Tito, N. B. Glass transition of polymers in bulk, confined geometries, and near interfaces. *Reports on Progress in Physics* **2017**, *80*, 036602.

(40) Napolitano, S.; Wübbenhorst, M. The lifetime of the deviations from bulk behaviour in polymers confined at the nanoscale. *Nature Communications* **2011**, *2*, 260.

(41) George, G.; Kriuchevskyi, I.; Meyer, H.; Baschnagel, J.; Wittmer, J. P. Shear-stress relaxation in free-standing polymer films. *Phys. Rev. E* **2018**, *98*, 062502.

(42) Bonn, D.; Eggers, J.; Indekeu, J.; Meunier, J.; Rolley, E. Wetting and spreading. *Rev. Mod. Phys.* **2009**, *81*, 739–805.

(43) Graziano, R.; Preziosi, V.; Uva, D.; Tomaiuolo, G.; Mohebbi, B.; Claussen, J.; Guido, S. The microstructure of Carbopol in water under static and flow conditions and its effect on the yield stress. *Journal of Colloid and Interface Science* **2021**, *582*, 1067 – 1074.

(44) Elder, R. M.; Knorr, D. B.; Andzelm, J. W.; Lenhart, J. L.; Sirk, T. W. Nanovoid formation and mechanics: a comparison of poly(dicyclopentadiene) and epoxy networks from molecular dynamics simulations. *Soft Matter* **2016**, *12*, 4418–4434.

(45) Miccio, L.; Cimmino, F.; Kurelac, I.; Villone, M. M.; Bianco, V.; Memmolo, P.; Merola, F.; Mugnano, M.; Capasso, M.; Iolascon, A.; Maffettone, P. L.; Ferraro, P. Per-

spectives on liquid biopsy for label-free detection of "circulating tumor cells" through intelligent lab-on-chips. *View* **2020**, *1*, 20200034.

(46) Lv, P.; Yang, Z.; Hua, Z.; Li, M.; Lin, M.; Dong, Z. Measurement of viscosity of liquid in micro-crevice. *Flow Measurement and Instrumentation* **2015**, *46*, 72 – 79.

(47) Kume, E.; Baroni, P.; Noirez, L. Strain-induced violation of temperature uniformity in mesoscale liquids. *Scientific Reports* **2020**, *10*, 13340.

(48) Do, J.-L.; Friščić, T. Mechanochemistry: A Force of Synthesis. *ACS Central Science* **2017**, *3*, 13–19, PMID: 28149948.

(49) Howard, J. L.; Cao, Q.; Browne, D. L. Mechanochemistry as an emerging tool for molecular synthesis: what can it offer? *Chem. Sci.* **2018**, *9*, 3080–3094.

(50) van Galen, M.; van der Gucht, J.; Sprakel, J. Chemical Design Model for Emergent Synthetic Catch Bonds. *Frontiers in Physics* **2020**, *8*, 361.

(51) Klein, I. M.; Husic, C. C.; Kovács, D. P.; Choquette, N. J.; Robb, M. J. Validation of the CoGEF Method as a Predictive Tool for Polymer Mechanochemistry. *Journal of the American Chemical Society* **2020**, *142*, 16364–16381, PMID: 32902274.

(52) Michels, L.; Gorelova, V.; Harnvanichvech, Y.; Borst, J. W.; Albada, B.; Weijers, D.; Sprakel, J. Complete microviscosity maps of living plant cells and tissues with a toolbox of targeting mechanoprobes. *Proceedings of the National Academy of Sciences* **2020**, *117*, 18110–18118.

(53) Hickenboth, C. R.; Moore, J. S.; White, S. R.; Sottos, N. R.; Baudry, J.; Wilson, S. R. Biasing reaction pathways with mechanical force. *Nature* **2007**, *446*, 423–427.

(54) Konda, S. S. M.; Brantley, J. N.; Bielawski, C. W.; Makarov, D. E. Chemical reactions modulated by mechanical stress: Extended Bell theory. *The Journal of Chemical Physics* **2011**, *135*, 164103.

(55) Konda, S. S. M.; Avdoshenko, S. M.; Makarov, D. E. Exploring the topography of the stress-modified energy landscapes of mechanosensitive molecules. *The Journal of Chemical Physics* **2014**, *140*, 104114.

(56) Roessler, A. G.; Zimmerman, P. M. Examining the Ways To Bend and Break Reaction Pathways Using Mechanochemistry. *The Journal of Physical Chemistry C* **2018**, *122*, 6996–7004.

Graphical TOC Entry

Some journals require a graphical entry for the Table of Contents. This should be laid out "print ready" so that the sizing of the text is correct.
Inside the `tocentry` environment, the font used is Helvetica 8 pt, as required by *Journal of the American Chemical Society*.
The surrounding frame is 9 cm by 3.5 cm, which is the maximum permitted for *Journal of the American Chemical Society* graphical table of content entries. The box will not resize if the content is too big: instead it will overflow the edge of the box.
This box and the associated title will always be printed on a separate page at the end of the document.